International Journal of ChemTech Research
CODEN (USA): IJCRGG ISSN: 0974-4290
Vol.8, No.3, pp 1189-1202, 2015

Room temperature cigarette smoking sensing performance of nanostructured SnO_2 thin films

R. H. Bari[1]*, S. B. Patil[1]

[1]Nanomaterials Research Laboratory, Department of Physics, G. D. M. Arts, K. R. N. Commerce and M.D. Science College, Jamner 424 206, Maharashtra, India

Abstract: The nanostructured SnO_2 thin films were prepared by spray pyrolysis technique. The cigarette smoke sensing performance of these films were systematically studied. The results reveal that the nanostructured SnO_2 sensor has enhanced sensing properties to 10–80 ppm cigarette smoke at room temperature. The instant response time (~16 s) and fast recovery (~21 s) are the main features of this sensor. To understand reasons behind this uncommon cigarette smoke sensing performance of the thin films, their structural, surface morphology, elemental composition, surface area electron diffaraction pattern, and microstructural properties were studied using X-ray diffraction(XRD), electron microscopy (FE-SEM and TEM), energy dispersive spectrophotometer (EDAX) respectively. Optical band gap energy match with reported band gap energy. The results are discussed and interpreted.
Keywords: Spray Pyrolysis, nanostructured SnO_2, cigarette smoke, analytical technique, gas response.

1. Introduction

A cigarette may look harmless enough - tobacco leaves covered in white paper. But when it is burn, it releases a dangerous cocktail chemicals including nicotine a highly addictive drug and many additives designed to make cigarettes taste nicer and keep smokers hooked. Some of these chemicals, like nicotine, are found naturally in the tobacco plant or absorbed by the plant from the soil, air and fertilizers. Cigarette smoke has proven to be a major health concern over the past years and it is a complex and reactive mixture containing chemicals that are both toxic and carcinogenic. The literature reveals that cigarette smoke contains more than 5000 chemicals including 90 ingredients that are hazardous [1]. Passive smoking is equally dangerous; non-smokers who breathe in this second hand smoke containing nicotine and other harmful substances on regular basis are susceptible to toxic effects that are absorbed into the body [2].Tobacco smoke is a varied, dynamic and reactive combination containing an estimated number of chemicals [3-5].The main ingredients being nicotine, tar and carbon monoxide. Nicotine is a tertiary amine composed of a pyridine and a pyrrolidine ring, this along with carbon monoxide and tar are known to have independent effects on the human body. This toxic and carcinogenic blend is probably the most major source of toxic chemical exposure and chemically mediated disease in humans [6].Literature has revealed that highly exposed nonsmokers and active smokers share the same level of hair nicotine [7]. Thus there is an urgent need to monitor cigarette smoking in free living conditions.

Semiconductor metal oxide (SMO) sensor technology is based on the change in resistance of a sensitive metal oxide layer which is induced by the interaction between a surface and ambient gases. Metal oxide semiconductors demonstrate good detection sensitivity, robustness and the ability to withstand high temperatures and the technique is commonly used to monitor a variety of toxic and inflammable gases in a

variety of air pollution monitoring systems, the food industry, medical diagnosis equipment and gas leak alarms. Since the last decade there has been a great deal of interest in the preparation of inexpensive thin films of SnO_2. This is because tin dioxide based thin films with large band gap ($Eg > 3$ eV) *n*-type semiconductors are attractive from the scientific and technological point of view [8]. SnO_2 posses excellent capability of exchange of oxygen from the atmosphere due to natural non- stoichiometry, that makes it the most suitable material for gas sensing application. The adsorption/desorption of oxygen on the surface of SnO_2 is the key parameter for change in conductance. The adsorbed oxygen on the surface (or grain boundaries) of SnO_2 captures the free electrons and becomes O^{-2}. It is important to point out that chemisorption of oxygen is crucial for gas sensing mechanism. Gas sensing applications demand materials at a quick response-recovery time and high response for trace level detection of various gases. Semi-conducting tin oxide is found useful for various gas sensing applications and improve its sensitivity and selectivity with appropriate catalysts [9].

A variety of technique have been employed to prepare nanostructure SnO_2 thin films. These includes spray pyrolysis [10], ultrasonic spray pyrolysis [11], chemical vapour deposition [12], activated reactive evaporation [13], ion-beam assisted deposition [14] and sol–gel[15] methods. Among these techniques, spray pyrolysis has proved to be simple, reproducible and inexpensive, as well as suitable for large area applications. Besides the simple experimental arrangement, high growth rate and mass production capability for large area coatings make them useful for industrial as well as solar cell applications. In addition, spray pyrolysis opens up the possibility to control the film morphology and particle size in the nanometer range. As demonstrated [16] spray pyrolysis is a versatile technique for deposition of metal oxides.

Fernandez et al studied the A.C. conductivity of SnO_2-CuO composites prepared by hydrothermal method and proposed it as a suitable material for detecting cigarette smoke [2]. Patil et al obtained Co- doped SnO_2 thin films by a conventional spray pyrolysis technique using stannic chloride and powder of cobalt acetate (volume ratio 1:4) as reactants and studied its CO (content of cigarette smoke) sensing properties as function of concentration and operating temperature [17].

In present investigation, we report nanostructured SnO_2 thin film prepared by spray pyrolysis technique at a substrate temperature of 250 ^oC with different spraying time of the solution. For the first time, the experimental results indicate that the nanostructured SnO_2 thin film was good sensing material for detecting cigarette smoke at room temperature (40 ^0C) with low concentration 50 ppm. The effect of spraying time of the solution on structural, surface morphology, microstructural, and cigarette smoke sensing properties were studied and investigated.

2. Experimental details

2.1. Preparation of nanostructured SnO_2 films

Nanostructured SnO_2 films were prepared on preheated glass substrate using a spray pyrolysis technique. Spray pyrolysis is basically a chemical process, which consists of a solution that is sprayed onto a hot substrate held at high temperature, where the solution reacts to form the desired thin film.

The spraying solution was prepared by mixing the appropriate volumes of 0.05 M Tin (II) chloride dehydrate ($SnCl_2.2H_2O$), Purified Merck) in de-ionized water as a precursor. The SnO_2 films were deposited at different spraying time of: 10 min, 20 min, 30 min and 40 min were obtained and referred to as S1, S2, S3 and S4 respectively. The optimized values of important preparative parameters are shown in table 1. Spray rate (7 ml/min), distance between substrate to nozzle (30 cm), solution concentration (0.05 M). The deposition process needs fine droplets to react on the heated substrate, owing to the pyrolytic decomposition of the solution. The hot substrate provides the thermal energy for the thermal decomposition and subsequent recombination of the constituent species. After the deposition, the films were allowed to cool naturally at room temperature. All the films were adherent to the substrate, were further used for structural, morphological, and microstructural characterizations. The pyrolytic reaction takes place on a heated substrate, leading to a nanostructured SnO_2. The usual expression for this reaction is:

$$SnCl_4.\ 5H_2O \rightarrow SnO_2 + 3H_2O \uparrow + 4HCl \uparrow \qquad \text{------- (1)}$$

2.2. Optimized parameters

Table 1 shows the optimized parameters for the preparation of nanostructured SnO_2 thin films

Table 1. Optimum parameter to obtain nanostructured SnO_2 thin films

Spray parameter	Optimum value / item
Nozzle	Glass
Nozzle to substrate distance	30 cm
$SnCl_2.2H_2O$ solution concentration	0.05 M
Solvent	De-ionised water
Solution flow rate	7 ml/ min.
Carrier gas	Compressed air
Substrate deposition temperature	250 ^{0}C
Spray deposition time	10 min, 20 min, 30 min, and 40 min

2.3. Annealing of SnO_2 thin films

The as prepared nanostructured SnO_2 thin film samples S1, S2, S3 and S4 were annealed at 500 ^{o}C for 1 h.

3. Thin films characterizations

The structural analysis of nanostructured SnO_2 thin films was carried out by X-ray diffraction (Miniflex Model, Rigaku, Japan) using CuKα radiation with a wavelength, λ = 1·5418 Å. The surface morphology and constituents of elements were estimated by means of field emission scanning electron microscope equipped with energy dispersive spectrophotometer (FE-SEM, JEOL. JED 6300). Microstructure property and surface area electron diffraction patterns of nanostructured SnO_2 thin films were obtained by using transmission electron microscopy (TEM) [CM 200 Philips (200 kV HT)]. Optical band gap studies were conducted using UV–VIS absorption spectroscopy (Shimadzu 2450 UV-VIS).The thickness of thin films were measured by weight difference method. Electrical conductivity and cigarette smoke sensing performance were studied using a static gas sensing system at various concentration with different operating temperature.

4. Results and discussion

4.1. X-ray diffraction analysis

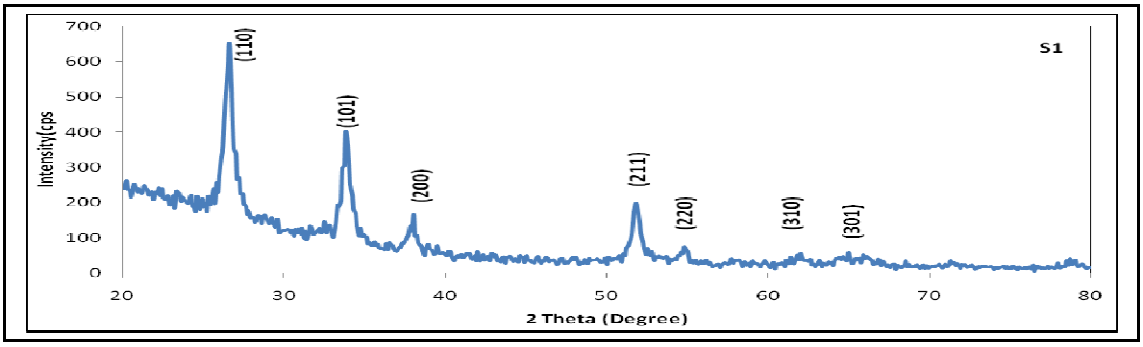

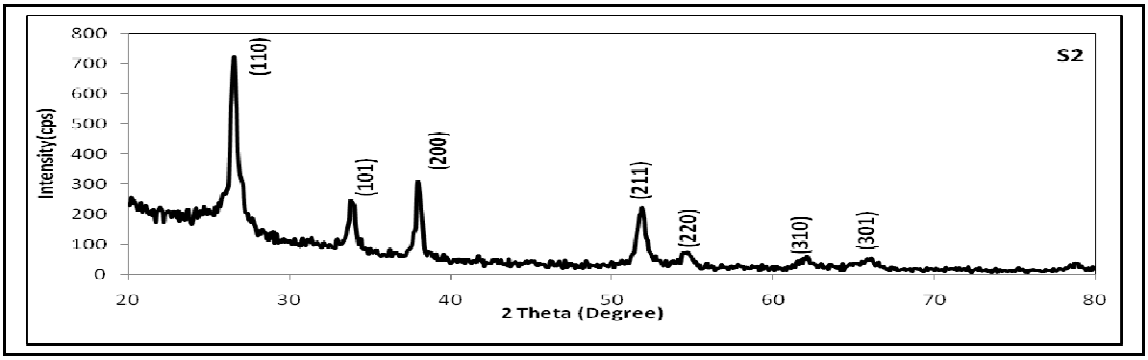

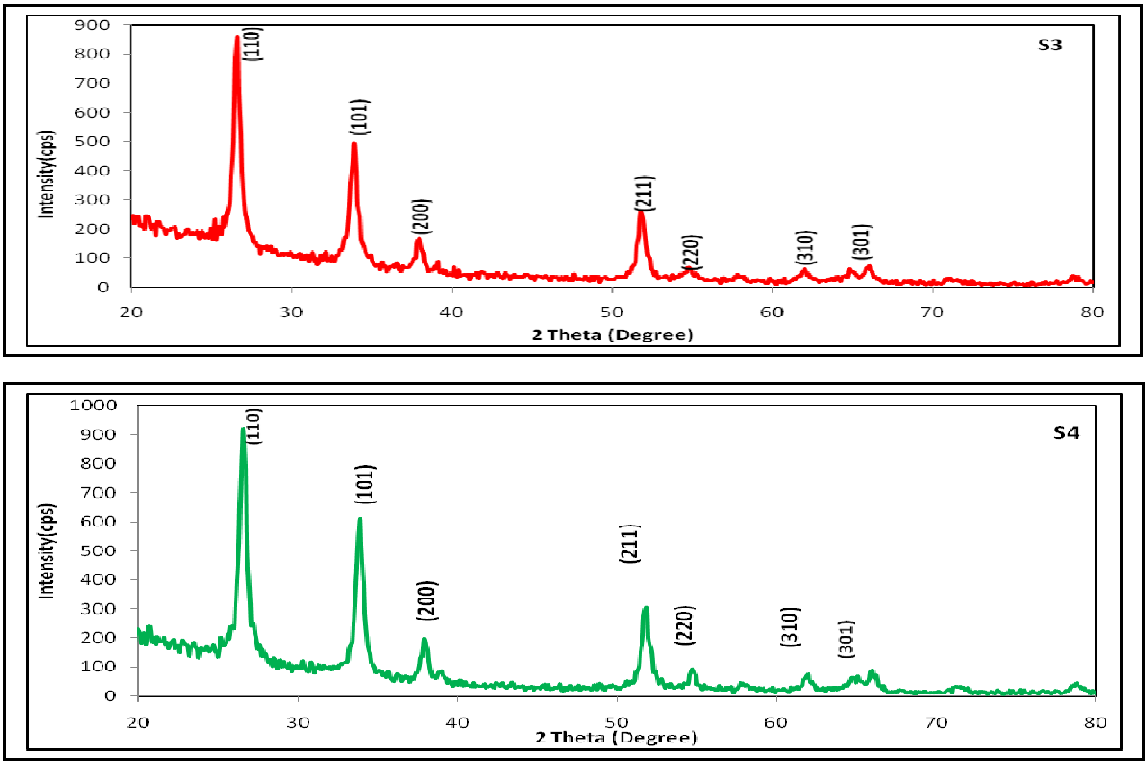

Figure 1. X-ray diffractogram of nanostructured SnO_2 thin films samples: S1, S2, S3 and S4.

The X-ray diffraction pattern of thin film samples at different spray deposition time is shown in Figure 1. The XRD spectrum shows a number of well-defined diffraction peaks. All the films shows tetragonal structure of nanostructured SnO_2 thin films with preferred orientation along the planes (110), (101), (200), (211), (220), (310) and (301). The peaks in the XRD are match well in agreement with the standard JCPDS data of pure SnO_2 (JCPDS data Card no. 21-1250). The average crystallite size of tin oxide thin film samples were calculated by using the Scherrer equation

$D = 0{\cdot}9\lambda/\beta\cos\theta$ ----------(2)

Where, D = Average crystallite size

λ = X-ray wavelength (1·5418 Å)

β = FWHM of the peak

θ= Diffraction peak position.

The calculated crystallite sizes were found between 19 to 33 nm. It has been reported by Amma et al [18] with increasing the spray deposition time does not affect the preferred orientational growth of the films and the locations of the measured diffraction peaks do not change significantly but intensities of the peaks increases with spray rate. Extended spray deposition time helps to accumulate more oxygen in the structure. This is due to the crystallinity of the films being improved and crystallite size becoming larger when elevating the spray rate. In this study, the films have good quality of crystallinity with increasing spray deposition time.

4.2. Surface Morphology

The morphology of the prepared film was analyzed using a field emission scanning electron microscope (FE-SEM, JEOL. JED 6300) Figure 2(a)–(d) shows the FESEM images, showing surface topography of S1, S2, S3 and S4 thin film samples respectively. The morphology of the grains was roughly spherical in shape. Thus the grain size goes on increasing with the increase in spraying time of the solution. In Fig. 2 (a), (b) and (c) grains are uniformly distributed and Fig.2 (d) show agglomeration of grains. It may be due to collapse of larger grains into smaller with the increase of spraying time of the solution. The observed grain sizes were found between 17 to 30 nm.

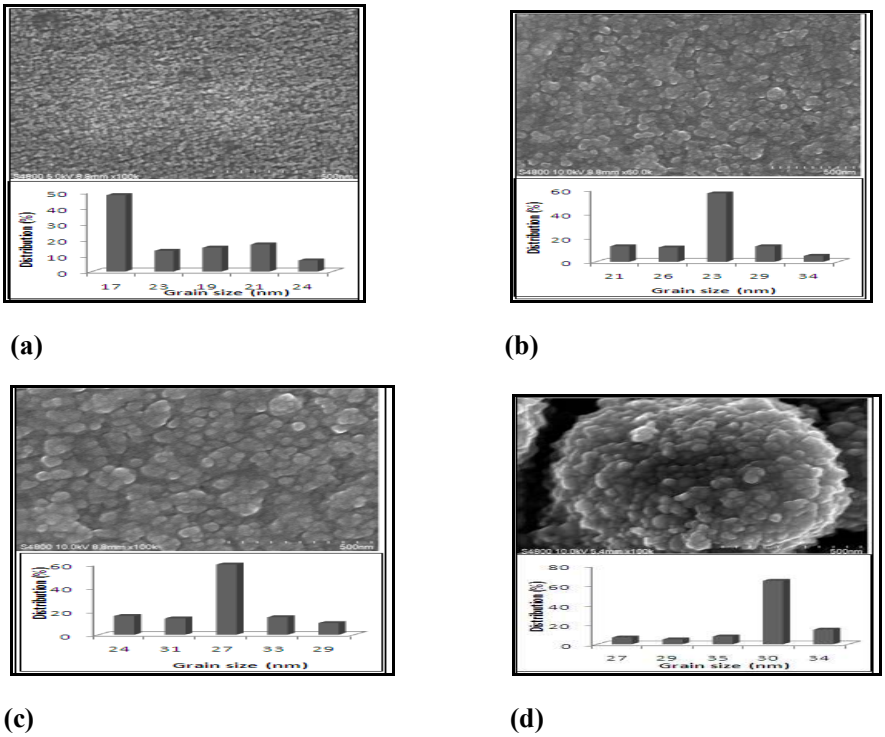

Figure 2. FE-SEM images of nanostructured SnO_2 thin film samples with histogram to indicate grain size distribution: (a) S1, (b) S2, (c) S3 and (d) S4.

4.3. Microstructured property and surface area electron diffraction pattern using TEM

TEM images and the corresponding electron diffraction pattern for nanostructured SnO_2 are shown in figures 3 and 4, respectively. The morphology and microstructure of SnO_2 thin films were investigated from TEM images. All the samples were scanned in all zones before the picture was taken. The micrographs showed that the grains were nearly spherical and the crystallite size distribution was in the range from 18 to 34 nm.

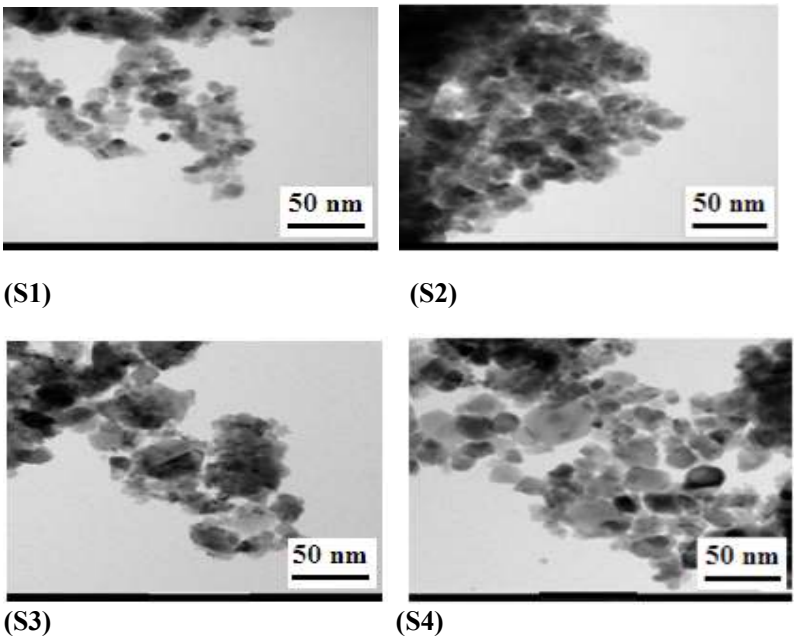

Figure 3. TEM images of nanostructured SnO_2 thin film sample: S1, S2, S3 and S4

The electron diffraction pattern of sample S2 (most sensitive sample) shows spotty but continuous ring patterns without any additional diffractions pots and rings of secondary phases, revealing their highly crystalline structure.

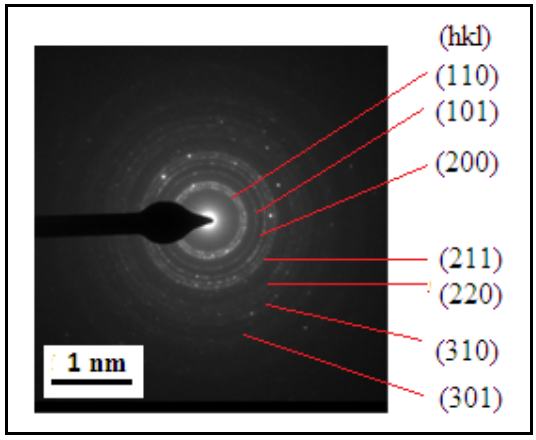

Figure 4. Electron diffraction pattern of nanostructured SnO_2 thin film sample (most sensitive sample=S2)

The electron diffraction patterns show clear and continuous ring patterns revealing their polycrystalline structure. Seven fringe patterns corresponding to planes: (110), (101), (200), (211), (220), (310) and (301) were consistent with the peaks observed in XRD patterns. XRD and TEM studies confirmed pure tetragonal structure of SnO_2 as evidenced from figures 1 and 4, respectively.

4.4. Quantitative elemental analysis (EDAX)

Figure 5 shows the elemental analysis of nanostructured SnO_2 thin film. It was analyzed using an energy dispersive spectrophotometer. The quantitative elemental analysis of the as deposited SnO_2 films was carried out at room temperature.

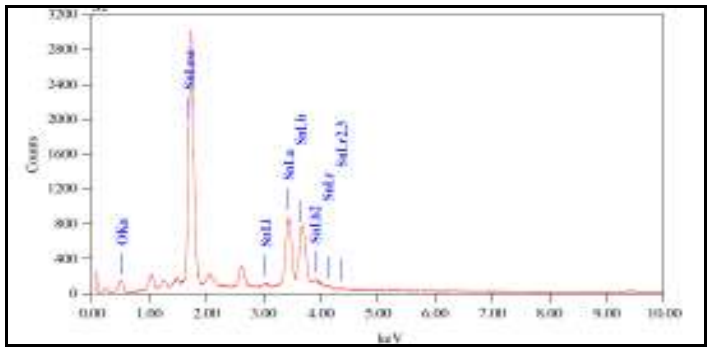

Figure 5. Elemental analysis of nanostructured SnO_2 thin film sample (S2)

Table 2. Quantative elemental analysis as prepared nanostructured SnO_2thin film

Sample No.	Sn (at%)	O (at%)	Remarks
S1	31.78	68.22	Nonstoichiometric
S2	30.37	69.63	Nonstoichiometric
S3	28.76	71.24	Nonstoichiometric
S4	27.24	72.76	Nonstoichiometric

Stoichiometrically expected at% of Sn and O is 33.30: 66.70. The observed at% of Sn and O were presented in Table 2. It is clear from table 2 that as prepared nanostructured SnO_2 thin films were observed to be nonstichoimetric in nature.

4.5 Optical band gap analysis using UV-spectroscopy

Optical absorption studies of nanostructured SnO_2 thin films were carried out in the wavelength (λ) range 250-650 nm at room temperature. The variation of absorbance with wavelength (λ) as shown in Fig. 6.

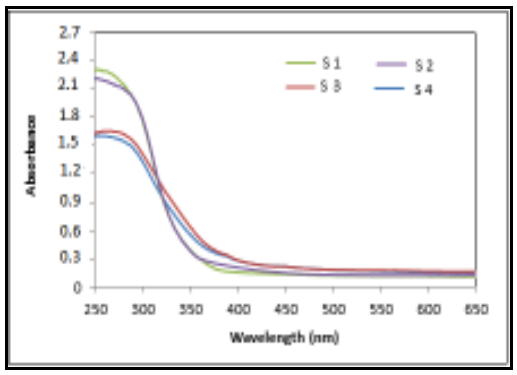

Figure 6. The variation of absorbance with wavelength (nm) for nanostructured SnO_2 thin film samples: S1, S2, S3 and S4.

The band gap energies of the samples were calculated from the absorption edges of the spectra [19]. The slope drawn from the start of an absorption edge (the onset of absorbance) and horizontal tangent had drawn on absorption minimum and intercepted each other at some point.

The vertical line drawn from this point on wavelength axis gave the absorption edge wavelength. This value of λ (nm) was then used in the following relation to know band gap energy:

$$Eg = h\nu = h\,c/\lambda = (1240)/\lambda\ (nm)\ eV \quad \text{----------(3)}$$

Calculated band gap energy are in the range of S1=3.82, S2=3.76, S3= 3.61 and 3.56. The values of band gap energies are matching approximately with the reported band gap energy 3.6 eV [20].

There is decrease in band gap as the spraying time is increasing from: 10 min. to 40 min. Spraying time is directly related with the thickness of the film. Longer the spraying time interval is, thicker the film. Crystallite size has a direct dependence on the film thickness. It has been observed that the crystallite size increases with an increase of the film thickness [21]. The decrease of band gap may be due to nanocrystalline nature of the films.

4.6. Determination of film thickness

The film thickness was measured by a weight difference method [22].In order to measure the thickness of the thin films by using weight difference method, error and accuracy was found to be ± 5 % nm. The thickness, sample weight and sample area are related as:

$t = M/A.\rho$ ---------- (4)

Where, M is the weight of the sample in gm,

A the area of the sample in cm^2

and ρ the materials density in gm cm^{-3}.

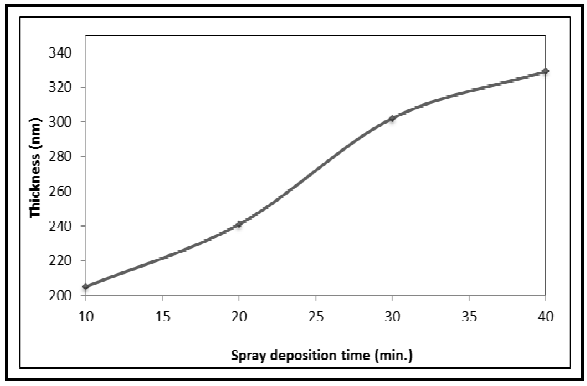

Figure 7. Variation of spray depostion time with thickness of the films (nm)

The variation of thickness of the deposited films and spray depostion time is shown in Fig.7. from which, It is observed that the spray deposition time goes on increasing, the thickness of the film increases, attains 329 nm value at 40 min. (spray deposition time).At initial condition spraying time (10 min.) of the solution is low, resulting in lower thickness 205 nm. As the spraying time increases, thickness increases continuously due to relative increase in Sn^{4+} ions in the solution [23].

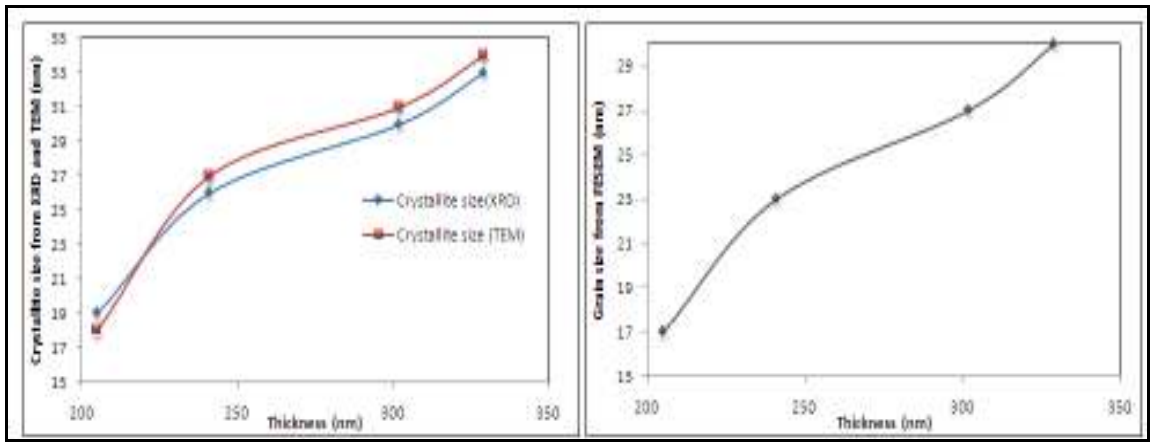

Figure 7. (a) and (b). Variation of crystallite size (from XRD and TEM), and grain size (FE-SEM) as function of thickness of the films

From Fig. 7 (a) and (b**)** it is clear that the crystallite size (calculated and observed from XRD and TEM) and grain size (FE-SEM) associated with the thin films an increase with increase in film thickness. This indicate that the film thickness contribute to the improvement in crystallinity with film thickness. Crystallinity of the material is direct dependence on the film thickness. Crystallinity has been observed to improve with an increase of the film thickness [24]. Moreover, the increase of crystallite size could be attributed to the improvement of the crystallinity and an increase in the cluster formation leading to agglomeration of small crystallites. These agglomerated crystallites coalesce together resulted in the formation of larger crystallites with better crystallinity.

5. Electrical properties

5.1. I–V characteristics

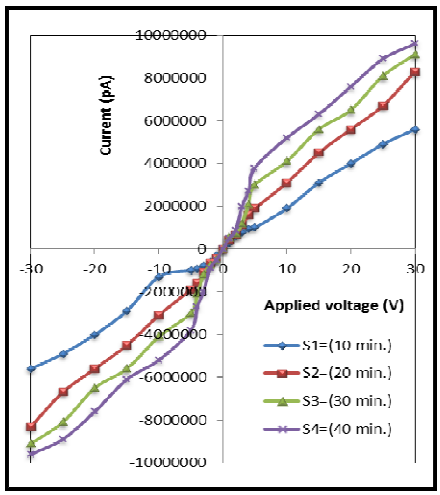

Figure 8. I–V characteristics of nanostructured SnO_2 thin film sensors.

In air, I – V characteristics of nanostructured SnO_2 films are shown in figure 8 increase nearly linear relationship curve was noted for positive (5 to 30 V) and negative (-5 to -30 V) applied bias voltages. The contacts were made by silver paste on thin film surface. The configuration was 1.5 cm × 1 cm. The graphs are

observed to be symmetrical in nature indicating ohmic contact. Confirmation of ohmic contacts would ensure that the change in resistance could only be due to the influence of gas exposure.

5.2. Electrical conductivity

Figure 9 shows the variation of log (σ) with operating temperature. The conductivity of each sample is observed to be increasing with an increase in temperature range between 293 ^{o}K and 373 ^{o}K in steps of 20 ^{o}K. The increase in conductivity with increase in temperature could be attributed to negative temperature coefficient of resistance and semiconducting nature of nanostructured SnO_2.

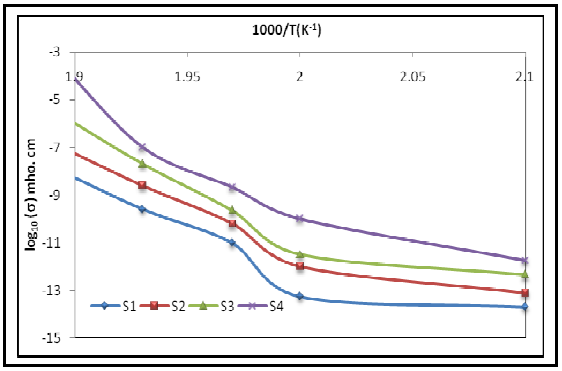

Figure 9. Variation of log (σ) with reciprocal of operating temperature (^{o}K).

This can be attributed to the generation of electrons due to thermal excitation. However, some of these electrons from the conduction band of SnO_2 are extracted by the oxygen adsorbed on the surface of the semiconductor [25], hence increasing the resistance of the semiconductor. The adsorbed oxygen undergoes the following reactions [26]:

$O_2 + e^- = O_2^-$ and $O_2 + e^- = 2O^-$----------(5)

Thus, the equilibration of the chemisorptions process results in the stabilization of surface resistance. Any process that disturbs this equilibrium gives rise to changes in the conductance of

semiconductors [25]. It clearly indicates that the nanostructured SnO_2 thin films were semiconducting in nature.

It is reported [27] as the thickness of the film increases activation energy goes on decreasing. Electrical conductivity was calculated using the relation:

$\sigma = \sigma_o \exp(-\Delta E/kT)$ ---------- (6)
Where, σ = conductivity
σ_o = conductivity constant
k = Boltzmann constant
T = Temperature

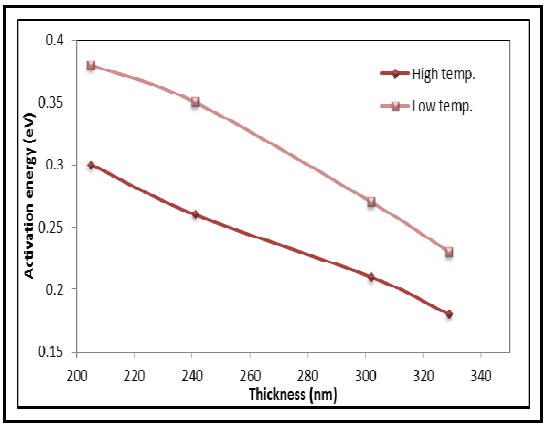

Figure 10. Variation of activation energy (ΔE) with thickness (nm)

In Figure 10 the activation energy is calculated from slopes of line for sample S1, S2, S3 and S4 thin films. It is clear from figure 10 that, as film thickness of the sample goes on increasing; the activation energy goes on decreasing. The decrease in activation energy with increasing film thickness may be due to the change in structural parameters, improvement in crystalline and grain size [28].

6. Gas sensing performance of the sensors

The gas sensing studies were carried out using a static gas chamber to sense cigarette smoke in air ambient and the experimental set up is described elsewhere [29]. The nanostructured SnO_2 thin films were used as the sensing elements. Cr-Al thermocouple is mounted to measure the temperature. The output of thermocouple is connected to temperature indicator. Gas inlet valve fitted at one of the ports of the base plate. The air was allowed to pass into the glass chamber before start of every new gas exposure cycle. Gas concentration (50 ppm) inside the static system is achieved by injecting a known volume of test gas in gas injecting syringe. The conductance of the sensor in dry air was measured by means of conventional circuitary by applying constant voltage (5 V) and measuring the current by picoammeter. The conductance was measured both in the presence and absence of test gas.

The gas response (S) is defined as the ratio of change in conductance in gas to air to the original conductance in air.

$S = G_g - G_a / G_a$ ---------- (7)
Where, G_a = the conductance of the sensor in air
G_g = the conductance on exposure of a target gas.

6.1. Cigarette smoke response

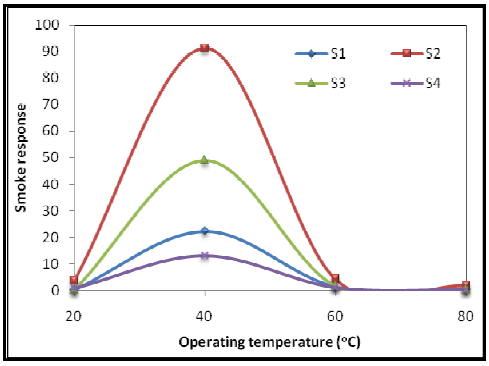

Figure 11. Cigarette smoking response of nanostructured SnO_2 thin films with operating temperature.

Figure 11 shows the variation in smoke response with the operating temperature to 50 ppm concentration of cigarette smoke for S1, S2, S3, and S4 samples. From Figure 11, it is found that cigarette smoke response increases with increase in operating temperature and shows maximum peak values at certain temperatures called optimal temperature and then decreases with further increase in temperature. At the optimal temperature, the activation energy may be enough to complete the chemical reaction. The observed increase and decrease in the cigarette smoke response indicates the adsorption and desorption phenomenon of the gases. The optimal temperature was confirmed for each SnO_2 film samples for four cycles. For cigarette smoke, the response was observed to increase with operating temperature up to 40°C .The resulting equation is-

$$O_2\,(atm) + 2e^-\,(cond\ band) \longrightarrow 2O^-(ads) \text{ ----------(8)}$$

After 40 °C temperature the surface would be unable to oxidize the gas so intensively Thus, the cigarette smoke response decreases with increasing temperature [30, 31].

6.2. Response and recovery of the sensor with repeatability of sensor

Fig. 12 shows the gas response against cigarette smoke concentration at 40 ^oC. It is observed that the response increases linearly as the cigarette smoke concentration increases from 10 to 50 ppm. From the graph, it is clear that with increase in the smoke concentration, the sensitivity increases reaching a saturation value at

very high concentrations. The saturation in the sensitivity can be attributed to complete coverage of the film surface by cigarette smoke molecules [32]. Both the response time (16 sec.) and recovery times (21 sec.) are observed at lower operating temperatures. The negligible quantity of the surface reaction products and their high volatility explain the quick response and fast recovery to cigarette smoke.

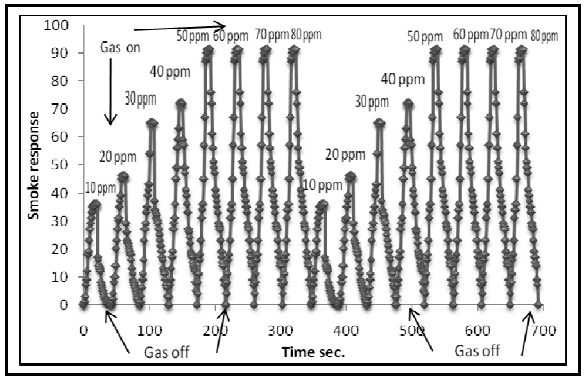

Figure 12. Response and recovery of the sensor with repeatability of sensor (most sensitive sample= S2).

6.3. Reproducible sensing cycles of SnO_2 thin films (S1, S2, S3 and S4)

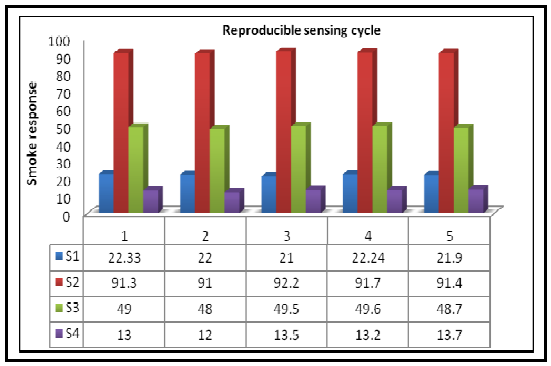

Figure 13. Repetition of cigarette smoke response for samples S1, S2, S3 and S4 at 40 ^{o}C.

Reproducible behaviour of each sample was tested by conducting 5 similar cycles of gas sensing process. The cigarette smoke response values of each sample was observed to be approximately similar as shown in Figure 13.

6.4. Reproducible sensing cycles

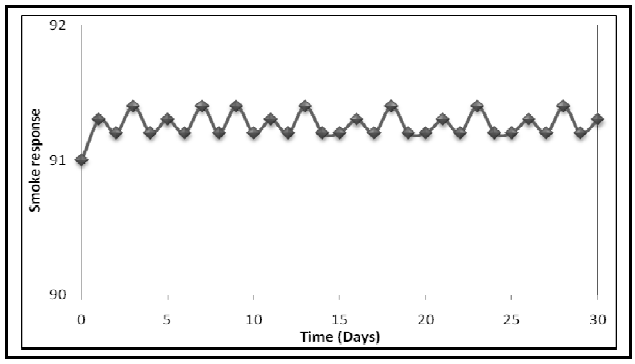

Figure 14. The long term stability studies for nanostructured SnO_2 (most sensitive sample=S2) thin film at an operating temperature of 40 ^{o}C.

The stability of the nanostructured SnO_2 sensor were measured by repeating the test many times (30 days). During the test, no significant variation was observed as shown in Fig. 14.The cigarette smoke selective

gas sensor had prominent long term stability in atmosphere for about 30 days. The obtained results show that both cigarette smoke response and electrical conductance were reproducible.

7. Discussion

7.1. Gas sensing mechanism

The nanostructured SnO_2 is oxygen deficient. Due to oxygen vacancies, the excess tin ions act as electron donors [11]. These electrons are captured by oxygen ions to get themselves adsorbed on the nanostructured SnO_2 surface. When cigarette smoke molecules are reduced, such as, and react with these negatively charged oxygen ions, the trapped electrons are given back to the conduction band of nanostructured SnO_2. The energy released during the decomposition of cigarette smoke molecules would be sufficient for electrons to jump up into the conduction band of SnO_2, causing an increase in the conductivity of the sensor as shown in Fig. 15.

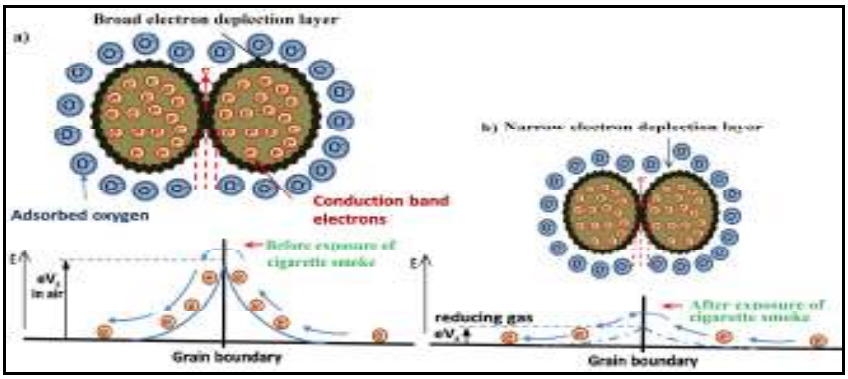

Figure 15. Gas-sensing mechanism of the nanostructured SnO_2 thin film sensor. (a) Before exposure and (b) after exposure of cigarette smoke.

The sensitivity of nanostructured SnO_2 thin film could be attributed to the high oxygen deficiency and defect density and leads to increased oxygen adsorption. The larger the amount of oxygen adsorbed on the surface, the larger the oxidizing capability will be and the faster the oxidation of gas will be [31, 33]. However, as shown in Figure 15(a), when nanostructured SnO_2 thin film consisting of nanograins in absence of cigarette smoke molecules, the depletion layer would extend throughout the entire layer of nanostructured SnO_2 on the film, and its resistance would become strikingly large. In a cigarette smoke molecules environment (see Figure 15(b)), the depleted layer would shrink quickly as it obtains conduction electrons due to reaction between cigarette smoke molecules adsorbed oxygen, and the resistance of the nanostructured SnO_2 would experience a large change.

8. Conclusions

Nanostructured SnO_2 thin films of various thickness were deposited, by varying the spray time of solution onto the glass substrates using a simple and inexpensive spray pyrolysis technique at 250 ^{0}C.XRD analysis confirmed that the prepared nanostructured SnO_2 thin films with tetragonal structure. FESEM and TEM image showed roughly spherical particles with nanostructured in nature. The EDAX of the film indicate that the films were nonstoichiometric. The value of crystallite size and grain size were observed to be increasing, optical band gap energy and activation energy decreasing with the increase of film thickness.SnO_2 thin film thin film based sensor structure have been designed for the trace level (50 ppm) detection of cigarette smoke at room temperatures (<40 ^{o}C) and exhibit the response of S= 91.3.Nanostructured SnO_2 films showed repeatable, reproducible and stability of sensor for cigarette smoke sensing performance. The nanostructured SnO_2 thin films exhibit rapid response–recovery which is one of the main features of this sensor.

Acknowledgements

The authors are thankful to the University Grants Commission, New Delhi for providing financial support. Thanks to Principal, G. D. M. Arts, K. R. N. Commerce and M.D. Science College, Jamner, for providing laboratory facilities for this work.

References

1. Reinskje Talhout, Thomas Schulz, Ewa Florek, Janvan Benthem, Piet Wester, Antoon Opperhuizen , Hazardous Compounds in Tobacco Smoke, Int J Environ Res Public Health, 2011, 8(2), 613-628.
2. A. C. Fernandez , P. Sakthivel , K. Saravana Kumar , J .Jesudurai , A New Approach towards Gas Sensing through A.C. Conductivity of Tin Oxide-Copper Oxide Composite, International journal of engineering sciences & research Technology, Jesudurai, 2014, 3(8),324-338.
3. D.Hoffmann, I. Hoffmann, Letters to the editor, tobacco smoke components. Beitr. Tabaksforsch. Int. 1998, 18, 49-52.
4. M Borgerding, H.Klus, Analysis of complex mixtures-cigarette smoke. Exp. Toxicol. Pathol. 2005, 57, 43-73.
5. Thielen A.; Klus H.; Muller, L. Tobacco smoke: unraveling a controversial subject. Exp. Toxicol. Pathol. 2008, 60, 141-156.
6. J.Fowles, E. Dybing, Application of toxicological risk assessment principles to the chemical constituents of cigarette smoke. Tob. Control, 2003, 12, 424-430.
7. H. Dimich-Ward, H.Gee, M.Brauer, V.Leung, Analysis of nicotine and cotinine in the hair of hospitality workers exposed to environmental tobacco smoke, JOccup Environ Med., 1997, 39(10),946-948.
8. V. Demarne, R. Sanjine, in: G. Sberveglieri (Ed.), Thin Film Semiconducting Metal Oxide Gas Sensors, Gas Sensors, Kluwer Academic Publishers, Netherlans, 1992, 89–116.
9. V. Gupta, S. Mozumdar, A. Chowdhuri, K. Sreenivas, Influence of CuO catalyst in the nano-scale range on SnO_2 surface for H_2S gas sensing applications, Pramana, 2005, 65, 647-652.
10. K. Murakami, K. Nakajima, S. Kaneko, Initial growth of SnO_2 thin film on the glass substrate deposited by the spray pyrolysis technique, Thin Solid Films, 2007,515, 8632-8636.
11. L.A. Patil, M.D. Shinde, A.R. Bari, V.V. Deo, Highly sensitive and quickly responding ultrasonically sprayed nanostructured SnO_2 thin films for hydrogen gas sensing, Sensors and Actuators B, 2009,143, 270-277.
12. T. Okuno, T. Oshima, S. Dong Lee, S. Fujita, Growth of SnO_2 crystalline thin films by mist chemical vapour deposition method, Physica status solidi (c), 2011, 8, 540-542.
13. H.S. Randhawa, M.D. Matthews, R.F. Bunshah, SnO_2 films prepared by activated reactive evaporation,Thin Solid Films, 1981, 83, 267-271.
14. T. Mohanty, Y. Batra, A .Tripathi, D. Kanjilal, Nanocrystalline SnO_2 formation using energetic ion beam, Journal of Nanoscience and Nanotechnololy, 2007, 7, 2036-2040.
15. J. Liu, S. Gong, J. Xia, L. Quan, H.Liu, D. Zhou, The sensor response of tin oxide thin films to different gas concentration and the modification of the gas diffusion theory, Sensors and Actuators B, 2009,138, 289-295.
16. P. S. Patil, Gas-chromism in ultrasonic spray pyrolyzed tungsten oxide thin films, Bulletin of Material Science, 2000, 23, 309-312.
17. S. B. Patil, M. A. More, A. V. Patil, Nanocrystalline Cobalt-doped SnO_2 Thin Film: A Sensitive Cigarette Smoke Sensor, Sensors & Transducers Journal, 2011, 134(11), 163-169.
18. D. S. D. Amma, V. K. Vaidyan, P. K. Manoj, Structural, electrical and optical studies on chemically deposited tin oxide films from inorganic precursors, Mater.Chem.Phy.,2005, 93 194-201.
19. R.H. Bari, L.A. Patil, R.H. Bari, L.A. Patil, Synthesis, characterization of bismuth selenide thin films by chemical bath deposition technique, Indian Journal of Pure & Applied Physics, 2010,48,127-132.
20. M. de la, L. Olvera, R. Asomoza, SnO_2 and SnO_2: Pt thin films used as gas sensors, Sens. Actuators B, 1997, 45,49.
21. J V.A. Chaudhary, I.S. Mulla, K. Vijayamohanan, Selective hydrogen sensing properties of surface functionalized tin oxide, Sens. Actuators B, 1999,55, 154–160.
22. R. H. Bari, S. B. Patil, Pervoskite nanostructured $CdSnO_3$ thin films as Cl_2 gas sensor operable at room temperature, Sensor letters, 2015, 13, 1-10.
23. A. V. Moholkar, S. M. Pawar, K. Y. Rajpure, C. H. Bhosale, Effect of concentration of $SnCl_4$ on sprayed fluorine doped tin oxide thin films, Journal of Alloys and compound, 2008, 455, 440-446.

24. L.A. Patil , M.D. Shinde, A.R. Bari, V.V. Deo, Highly sensitive and quickly responding ultrasonically sprayed nanostructured SnO_2 thin films for hydrogen gas sensing, Sens. Actuators B, 2002, 84,258-264.
25. B. D. Cullity, Elements of X-Ray Diffractions, (USA: Addison-Wesley Publishing Co.)1978, 36, 102
26. H. Windichmann and P. Mark, A model for the operation of a thin films conductance modulation carbondioxide sensor, J. Electrochem. Soc., 1979, 126, 627-633.
27. K. C. Sharma, J. C. Garg, Influence of thermal annealing in air on the electrooptic characteristic of chemical bath deposited non-stoichiometric cadmium zinc selenide thin films, Phys. D: Appl. Phys 1990, 23, 1411–1419.
28. R. H. Bari, S. B. Patil, A. R. Bari, Influence of precursor concentration of solution on CO sensing performance of sprayed nanocrystalline SnO_2 thin films, Optoelectronics and advanced materials–rapid communication, 2012, 6, 887-895
29. R. H. Bari , R. S. Khadayate, S. B. Patil, A. R. Bari, G. H. Jain, L. A. Patil , B. B. Kale, Preparation, characterization, and H_2S sensing performance of sprayed nanostructured SnO_2 thin films, ISRN Nanotechnology, 2012, 734325, 1-5.
30. D. R. Patil, L. A. Patil, G. H. Jain, M. S. Wagh, S. A. Patil, Surface activated ZnO thick film resistors for LPG gas sensing, Sensors & Transducers, 2006, 74, 874-883.
31. G. H. Jain, L. A. Patil, Gas sensing properties of Cu and Cr activated BST thick films, Bulletin of Material Science, 2006, 29, 403-411.
32. L.A. Patil, A.R. Bari, M.D. Shinde, Vinita Deo, Ultrasonically synthesized nanocrystalline ZnO powder-based thick film sensor for ammonia sensing, Sensor Review, 2010, 30, 290-296.
33. L.A. Patil, A.R. Bari, M.D. Shinde, Vinita Deo, D.P. Amalnerkar, Synthesis of ZnO nanocrystalline powder from ultrasonic atomization technique, characterization, and its application in gas sensing, IEEE Sensors, 2011, 11, 939-946.